N-(4-Hydroxyphenyl)retinamide increases dihydroceramide and synergizes with dimethylsphingosine to enhance cancer cell killing

Hongtao Wang,[1] Barry J. Maurer,[1] Yong-Yu Liu,[2] Elaine Wang,[3] Jeremy C. Allegood,[3] Samuel Kelly,[3] Holly Symolon,[3] Ying Liu,[3] Alfred H. Merrill, Jr.,[3] Valérie Gouazé-Andersson,[4] Jing Yuan Yu,[4] Armando E. Giuliano,[4] and Myles C. Cabot[4]

[1]Childrens Hospital Los Angeles, Keck School of Medicine, University of Southern California, Los Angeles, California; [2]College of Pharmacy, University of Louisiana at Monroe, Monroe, Louisiana; [3]School of Biology and Petit Institute of Bioengineering and Bioscience, Georgia Institute of Technology, Atlanta, Georgia; and [4]Gonda (Goldschmied) Research Laboratories at the John Wayne Cancer Institute, Saint John's Health Center, Santa Monica, California

Abstract

Fenretinide [*N*-(4-hydroxyphenyl)retinamide (4-HPR)] is cytotoxic in many cancer cell types. Studies have shown that elevation of ceramide species plays a role in 4-HPR cytotoxicity. To determine 4-HPR activity in a multidrug-resistant cancer cell line as well as to study ceramide metabolism, MCF-7/AdrR cells (redesignated NCI/ADR-RES) were treated with 4-HPR and sphingolipids were analyzed. TLC analysis of cells radiolabeled with [^{3}H]palmitic acid showed that 4-HPR elicited a dose-responsive increase in radioactivity migrating in the ceramide region of the chromatogram and a decrease in cell viability. Results from liquid chromatography/electrospray tandem mass spectrometry revealed large elevations in dihydroceramides (*N*-acylsphinganines), but not desaturated ceramides, and large increases in complex dihydrosphingolipids (dihydrosphingomyelins, monohexosyldihydroceramides), sphinganine, and sphinganine 1-phosphate. To test the hypothesis that elevation of sphinganine participates in the cytotoxicity of 4-HPR, cells were treated with the sphingosine kinase inhibitor D-erythro-*N*,*N*-dimethylsphingosine (DMS), with and without 4-HPR. After 24 h, the 4-HPR/DMS combination caused a 9-fold increase in sphinganine that was sustained through +48 hours, decreased sphinganine 1-phosphate, and increased cytotoxicity. Increased dihydrosphingolipids and sphinganine were also found in HL-60 leukemia cells and HT-29 colon cancer cells treated with 4-HPR. The 4-HPR/DMS combination elicited increased apoptosis in all three cell lines. We propose that a mechanism of 4-HPR–induced cytotoxicity involves increases in dihydrosphingolipids, and that the synergy between 4-HPR and DMS is associated with large increases in cellular sphinganine. These studies suggest that enhanced clinical efficacy of 4-HPR may be realized through regimens containing agents that modulate sphingoid base metabolism. [Mol Cancer Ther 2008;7(9):2967–76]

Introduction

One of the newer strategies for cancer treatment, as well as chemoprevention, is to modulate key signaling mediators and pathways to control the behavior of cancer cells. Sphingolipids are emerging as promising targets because this diverse family of compounds includes many subspecies (ceramides, sphingosine 1-phosphate, gangliosides, among other things) that regulate cell proliferation, differentiation, migration, and programmed cell death by both apoptotic and autophagic pathways (1–4). In addition, recent findings about the regulation of ceramide formation and turnover have opened new doors to understanding not only the basis for the toxic effects of sphingolipids on cancer cells but also the relationship between ceramide metabolism and multidrug resistance (5–7).

Ceramide species, the neutral lipid backbone of sphingolipids, have been known for some time to play a role in signaling apoptotic cell death (5, 8, 9), which is thought to be a major cytotoxic mechanism for many anticancer drugs (10, 11). Ceramides seem also to participate in cell death via other pathways such as autophagy (3, 4, 12). Important anticancer drugs such as anthracyclines, *Vinca* alkaloids, paclitaxel (Taxol), etoposide, and fenretinide, also referred to as *N*-(4-hydroxyphenyl)retinamide (4-HPR), have been reported to elevate ceramides by a variety of mechanisms. These include inducing ceramide synthesis *de novo*, activating turnover of sphingomyelin, and/or

Received 9/13/07; revised 6/13/08; accepted 6/25/08.

Grant support: USPHS Grants GM77391, CA95339, CA87525 and GM69338 (LIPID MAPS); Department of the Army DAMD 17-99-1-9228 (Postdoctoral Traineeship in Breast Cancer Research, to H.W.); Department of the Army DAMD 04-1-0491 (Postdoctoral Traineeship in Breast Cancer Research, to VG-A); The Susan G. Komen Breast Cancer Foundation, grant number BCTR0402450, and by funding from the Ben B. and Joyce E. Eisenberg Foundation (Los Angeles, CA), the Fashion Footwear Association of New York Charitable Foundation (New York, NY), Avon Foundation (New York, NY), the Association for Breast and Prostate Cancer Studies (Santa Monica, CA), Sandra Krause and William Fitzgerald (Los Angeles, CA).

The costs of publication of this article were defrayed in part by the payment of page charges. This article must therefore be hereby marked *advertisement* in accordance with 18 U.S.C. Section 1734 solely to indicate this fact.

Requests for reprints: Myles C. Cabot, Department of Experimental Therapeutics, John Wayne Cancer Institute, 2200 Santa Monica Boulevard, Santa Monica, CA 90404. Phone: 310-998-3924; Fax: 310-582-7325. E-mail: cabot@jwci.org, or Alfred H. Merrill, Jr., School of Biology, Georgia Tech, Atlanta, GA 30332-0230. Phone: 404-385-2842; Fax: 404-385-2917. E-mail: al.merrill@biology.gatech.edu

doi:10.1158/1535-7163.MCT-08-0549

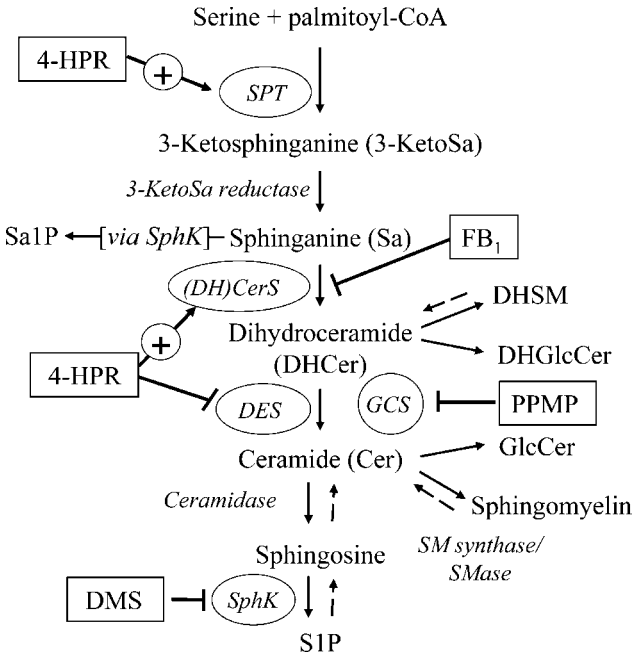

Figure 1. Ceramide metabolism with the sites of inhibitors. *SPT,* serine palmitoyltransferase; *(DH)CerS,* dihydroceramide synthase; *DES,* dihydroceramide desaturase; *SphK,* sphingosine kinase; *GCS,* glucosylceramide synthase; *Sa,* sphinganine; *DH,* dihydro-; Cer, ceramide; *SM,* sphingomyelin; *GlcCer,* glucosylceramide; *PPMP,* 1-phenyl-2-palmitoylamino-3-morpholino-1-propanol.

suppression of the conversion of ceramides into more complex sphingolipids as illustrated in Fig. 1 (reviewed in refs. 1, 4, 5).

Although ceramide produced for ''signaling'' involves the turnover of complex sphingolipids such as sphingomyelin, there is now a strong association between *de novo* ceramide biosynthesis and chemotherapy-induced apoptosis (1, 2, 13). The roles played by the enzymes that remove ceramides by metabolizing them into more complex sphingolipids were revealed during studies of cells refractory to chemotherapy (14–17) and led to the hypothesis that agents that modulate ceramide metabolism to sustain the apoptotic signal might improve the efficacy of chemotherapy (5). In this regard, blocking ceramide glycosylation with agents such as an inhibitor of glucosylceramide synthesis (1-phenyl-2-palmitoylamino-3-morpholino-1-propanol; Fig. 1) often enhances cytotoxicity (13–15, 18, 19). However, there is at least one exception that should be borne in mind: When ceramide is removed by hydrolysis to sphingosine and phosphorylated, this produces a compound, sphingosine 1-phosphate (S1P), which is associated with cell proliferation and survival (20).

In the present study, we describe findings with 4-HPR, an anticancer agent that has previously been shown to increase *de novo* sphingolipid biosynthesis by activation of serine palmitoyltransferase and dihydroceramide synthases (Fig. 1; ref. 21). 4-HPR imparts cytotoxic responses in many types of cancer cells (18) by increasing reactive oxygen species and ceramides and inducing apoptosis and/or mixed necrosis (22), although these may not be the only mechanisms of action of 4-HPR (23). By lipidomic analysis, using liquid chromatography/electrospray tandem mass spectrometry (LC MS/MS), of the subspecies of ceramides found in cells (i.e., variants in sphingoid base backbone and amide-linked fatty acids), as well as analysis of sphingolipids that are metabolically interconnected, we have determined that cells treated with 4-HPR displayed elevated dihydroceramide species rather than desaturated ceramides. In addition, there were substantial elevations in sphinganine and sphinganine 1-phosphate (Sa1-P). Due to the elevation in Sa1-P, which may be an antiapoptotic metabolite analogous to S1P, the combination of 4-HPR and the sphingosine kinase inhibitor D-erythro-*N,N*-dimethylsphingosine (DMS; Fig. 1) was tested. Experiments showed cytotoxic synergy when 4-HPR and DMS were combined at concentrations that were minimally cytotoxic as single agents. This cytotoxic synergy correlated with large increases in cellular sphinganine and dihydroceramides. These findings suggest that the efficiency of 4-HPR, and perhaps other agents that elevate dihydroceramides, may be enhanced by inhibiting sphingosine/sphinganine kinase activity to sustain elevation of sphingoid bases.

Materials and Methods

Cell Lines and Reagents

The ovarian carcinoma cell line MCF-7/AdrR, redesignated NCI/ADR-RES (24) and previously described as a breast cancer cell line, which is resistant to doxorubicin, was provided by Dr. Kenneth Cowan (University of Nebraska Medical Center Eppley Cancer Center, Omaha, NE) and Dr. Merrill Goldsmith (National Cancer Institute, Bethesda, MD). HT29, a human colon cancer cell line, and HL-60 cells, a human promyelocytic cell line, were obtained from the American Type Culture Collection. Cell culture media were from Invitrogen Corp., and characterized fetal bovine serum was from HyClone. C6-ceramide (*N*-hexanoylsphingosine), C6-dihydroceramide (*N*-hexanoyldihydro-sphingosine, D-*erythro*), DMS (D-erythro-*N,N*-dimethylsphingosine), sphinganine (D-erythro-dyhydrosphingosine), and myriocin were from BIOMOL. Myriocin was also purchased from Sigma Chemical and Calbiochem, and fumonisin B_1 (FB_1) was from Calbiochem. Ceramide and sphingomyelin (brain-derived) were from Avanti Polar Lipids, as was the internal standard cocktail for the mass spectrometric analysis. [9,10-^{3}H(N)]Palmitic acid (50 Ci/mmol) was from Dupont/NEN. Silica Gel G TLC plates (prescored) were from Analtech. 4-HPR was kindly provided by R.W. Johnson Pharmaceuticals but was also purchased from Sigma. GT11 {*N*-C8:0-cyclopropenylceramide, *N*-[(1*R*,2*S*)-2-hydroxy-1-hydroxymethyl-2-(2-tridecyl-1-cyclopropenyl)ethyl]octanamide}, a dihydroceramide desaturase inhibitor, was purchased from Matreya.

Cell Culture

Cell lines were cultured using conditions previously described. In brief, HL-60 (25) and MCF-7/AdrR cells (26) were cultured in RPMI 1640, and HT-29 cells were grown in DMEM (27). The media additionally contained 10% fetal bovine serum, 100 units/mL penicillin, 100 μg/mL streptomycin, and 584 mg/L L-glutamine. Cells were grown in a humidified 5% CO_2 tissue culture incubator at 37°C, and the adherent cell lines (all but HL-60) were released from the dishes for subculturing using 0.05% trypsin/0.53 mmol/L EDTA (Invitrogen).

Metabolic Radiolabeling and Analysis of Total Cellular (Dihydro)ceramides by TLC

Cells were radiolabeled in mid-log phase growth by addition of [^{3}H]palmitic acid (1.0 μCi/mL medium) for the times specified in the figure legends. After removal of the culture medium, cells were washed with PBS and the lipids were recovered from the dish by addition of ice-cold 2% acetic acid in methanol, followed by scraping of the cells from the dish with a plastic scraper. The mixture was transferred to 1-dram glass vials with Teflon screw caps for lipid extraction by the method of Bligh and Dyer (28). After vortex mixing and centrifuging, the organic lower phase was removed and evaporated under a stream of nitrogen. The lipids were dissolved in chloroform/methanol (2:1), spotted on Silica Gel G TLC plates, and developed with a solvent system containing chloroform/acetic acid (90:10, v/v). A commercial ceramide standard was co-chromatographed and visualized with iodine vapor. The corresponding region of the TLC plate (composed of both [^{3}H]dihydroceramides and [^{3}H]ceramides) was scraped and transferred to scintillation vials with 0.5 mL of water and 4.5 mL of EcoLume. Quantitation of tritium was by liquid scintillation counting with correction for quenching (which was minimal).

Sphingolipidomic Analysis by LC MS/MS

The sphingolipids were extracted and analyzed by the method of Merrill et al. (29) as briefly described here. After transfer of the cells to 13 × 100 mm borosilicate test tubes, a cocktail of sphingolipid internal standards (C17-sphingosine, C17-sphinganine, C17-sphingosine 1-phosphate, and C17-sphinganine 1-phosphate, C12-ceramide, C12-ceramide 1-phosphate, C12-glucosylceramide, C12-lactosylceramide, and C12-sphingomyelin) from Avanti Polar Lipids was added, and the lipids were

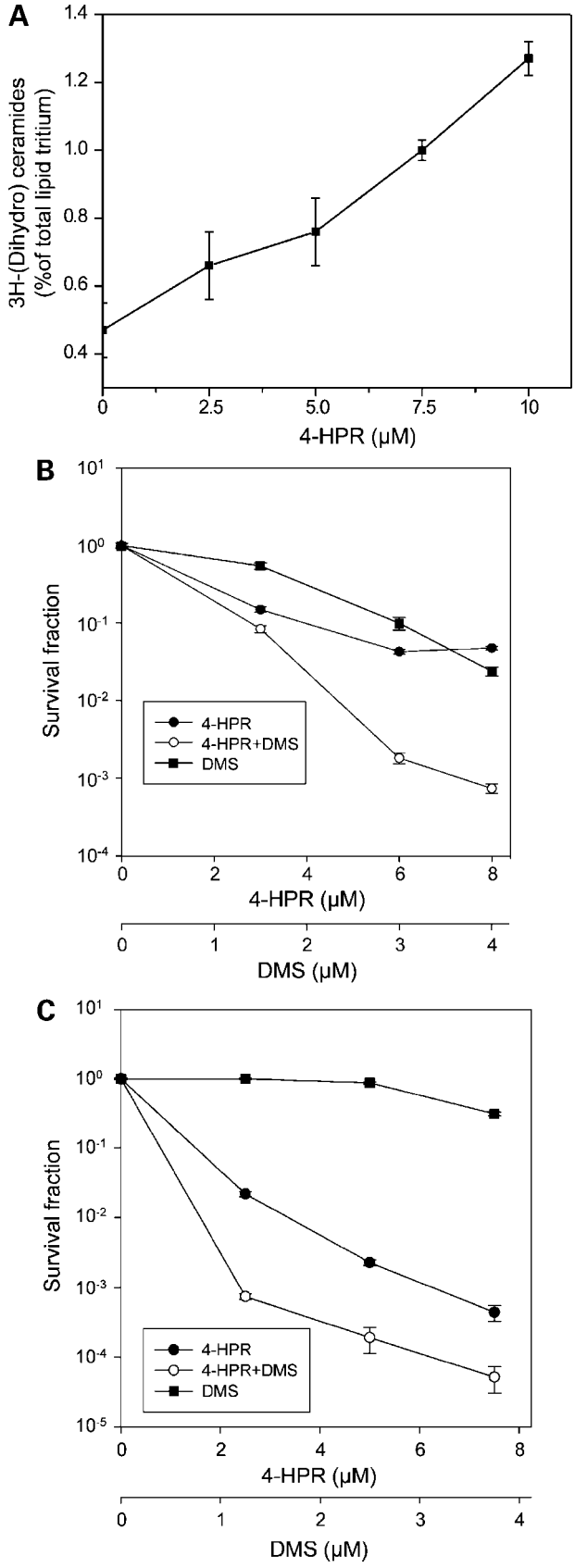

Figure 2. Effects of 4-HPR on [^{3}H](dihydro)ceramide formation in MCF-7/AdrR ovarian cancer cells and on cytotoxicity in the absence and presence of DMS in MCF-7/AdrR and HL-60 cells. **A,** MCF-7/AdrR cells were cultured with [^{3}H]palmitic acid and the 4-HPR concentrations indicated for +24 h. Lipids were extracted and analyzed by TLC. Cytotoxicity in MCF-7/AdrR (**B**) and HL-60 (**C**) cells was determined after +72 h by DIMSCAN. Ethanol was used as vehicle for 4-HPR and DMS. *Bars,* SD. MCF-7/AdrR cells: 3 μmol/L 4-HPR + 1.5 μmol/L DMS (combination index, 1.2); 6 μmol/L 4-HPR + 3 μmol/L DMS (combination index, 0.6); 8 μmol/L 4-HPR + 4 μmol/L DMS (combination index, 0.6); 10 μmol/L 4-HPR + 5 μmol/L DMS (combination index, 0.8). HL-60 cells: 2.5 μmol/L 4-HPR + 1.25 μmol/L DMS (combination index, 0.57); 5 μmol/L 4-HPR + 2.5 μmol/L DMS (combination index, 0.85); 7.5 μmol/L 4-HPR + 3.75 μmol/L DMS (combination index, 0.9).

Table 1. Influence of 4-HPR and DMS on sphingolipid metabolism in MCF-7-AdrR (NCI/ADR-RES) cells treated for extended times

Agents	Cell lipids (pmol 10^6 cells)			
	Ceramides	Sphinganine	Sphingosine	S1P
Control				
24 h	331	6.3 ± 1.5	55 ± 6.7	28.8 ± 8.8
48 h	878	17 ± 2.7	37.3 ± 13	77.7 ± 20
4-HPR				
24 h	934	38.3 ± 3.2	51 ± 11.5	10.5 ± 1.9
48 h	6,822	51.4 ± 3.0	18.4 ± 3.2	78.9 ± 32
DMS				
24 h	544	14.8 ± 0.6	6.3 ± 0.8	11.4 ± 1.3
48 h	1,515	27.6 ± 5.8	3.6 ± 1.0	60.9 ± 30
4-HPR/DMS				
24 h	1,478	54.9 ± 4.2	5.3 ± 0.5	9.2 ± 1.9
48 h	14,805	135.7 ± 29	2.2 ± 1.0	29 ± 7.8

NOTE: Cells (70% confluent) were treated with vehicle (ethanol), 4-HPR (5.0 μmol/L), DMS (5.0 μmol/L), or 4-HPR plus DMS for +24 and +48 h. Cells were then harvested for lipid analysis by LC MS/MS. The experiment was done in triplicate.

extracted and divided into two fractions that were applied to reverse-phase LC (for sphingoid bases) and normal-phase LC (for complex sphingolipids) coupled with electrospray MS/MS. The reverse-phase LC used a Supelco 2.1 mm i.d. × 5 cm Discovery C18 column and a flow rate of 1 mL/min. Mobile phase A consisted of $CH_3OH/H_2O/HCOOH$ (58:41:1; all mobile phase solvents are given in v/v); mobile phase B consisted of $CH_3OH/HCOOH$ (99:1); both also contained 5 mmol/L ammonium formate. For each analysis, the column was equilibrated with A/B (60:40) for 0.4 min; the sample was injected (50 μL by a Perkin-Elmer Series 200 Autosampler); A/B (60:40) was continued for 0.5 min, followed by a 1.8- min linear gradient to 100% B, which was held for 5.3 min; and then the column was reequilibrated at initial conditions for 0.5 min. The normal-phase LC used a Supelco 2.1 mm i.d. × 5 cm LC-NH_2 column and a flow rate of 1.0 mL/min. Mobile phase A consisted of $CH_3CN/CH_3OH/CH_3COOH$ (97:2:1); mobile phase B consisted of $CH_3OH/H_2O/CH_3(CH_2)_3OH/CH_3COOH$ (64:15:20:1); both also contained 5 mmol/L ammonium acetate. For each analysis, the column was equilibrated with A/B (98:2) for 0.5 min; the sample was injected; and A/B (98:2) was continued for 1.1 min, followed by a 0.2-min linear gradient to 82% A. This state is held for 0.4 min, followed by a 0.8-min linear gradient to 100% B and reequilibration of the column at initial conditions for 0.5 min.

The mass spectrometry data were collected using a PE Sciex ApI 3000 triple quadrupole mass spectrometer equipped with a turbo ion-spray source. Dry N_2 was used as the nebulizing gas at a flow rate of 6 L/min. The ionspray needle was held at 5,500 V, and the orifice and ring voltages were kept low (30–40 and 180–220 V, respectively) to minimize collisional decomposition of molecular ions before entry into the first quadrupole, and the N_2 drying gas temperature was set to 500°C. N_2 was used to collisionally induce dissociations in Q2, which was offset from Q1 by 30 to 40 V. Q3 was then set to pass molecularly distinctive product ions.

As the first step, each cell type was examined by product ion scans for *m/z* 264.4 and 266.4 through the (dihydro)ceramide and monohexosyl(dihydro)ceramide range and by precursor ion scans of *m/z* 184.4 for (dihydro)sphingomyelins to identify the major subspecies. With this information, a multiple reaction monitoring method has been developed for the fatty acyl chain length variants where each transition has a dwell time of ~25 ms. After building the multiple reaction monitoring protocol, the intensities of the signals for the different sphingolipid subspecies can be compared with the internal standards to arrive at estimations of the mass that are usually within ±10%.

For the analysis of the MCF-7/AdrR cells, dishes (10 cm) of cells at mid-log phase growth were treated for 24 and 48 h with 4-HPR (5.0 μmol/L), DMS (5.0 μmol/L), 4-HPR plus DMS, or vehicle (ethanol) in medium containing 5% fetal bovine serum. After rinsing in ice-cold PBS, cells were harvested with trypsin-EDTA and dispersed in serum-free medium for counting by hemocytometer or analysis of protein amount, then transferred to 13 × 100 mm borosilicate glass tubes and frozen at −80°C until analysis. HT-29 and HL-60 cells were treated with 10 μmol/L 4-HPR (or vehicle) and collected after 24 h.

Cytotoxicity and Apoptosis Assays

Cytotoxicity was determined after 72-h exposures using a fluorescence-based, digital imaging microscopy method (DIMSCAN) as described (18). Drug-induced cytotoxic synergy was analyzed by CalcuSyn software from Biosoft (18). By this method, a combination index equal to 1 indicates an additive effect, and combination indices of 0.7 to 0.85 and 0.3 to 0.7 indicate moderate synergism and synergism, respectively.

Apoptosis was evaluated on intact cultured cells after staining with SYTO-13 (Invitrogen) and propidium iodide. Cells were observed under an inverted fluorescent microscope (Olympus 1X70). With SYTO-13, normal nuclei exhibit a loose chromatin colored in green, and apoptotic nuclei exhibit condensed green-colored chromatin and/or fragmentation. Postapoptotic necrosis is denoted by condensed and/or fragmented nuclei, but orange colored.

Results

Initial experiments assessed the effect of 4-HPR on the biosynthesis of total ceramides, including dihydroceramides, and consequent cytotoxicity. As shown in Fig. 2A, when the cells were incubated with increasing concentrations of 4-HPR, there was a dose-dependent increase in the levels of [^{3}H](dihydro)ceramides generated. For example, [^{3}H](dihydro)ceramides were 0.47 ± 0.09% of the total ^{3}H-lipids in the control cells, whereas the percentage increased to 0.76 ± 0.1% (1.6-fold) and 1.27 ± 0.03% (2.7-fold) in cells treated with 5.0 and 10 μmol/L of 4-HPR,

respectively. We next evaluated 4-HPR cytotoxicity and determined whether DMS, a known sphingosine kinase inhibitor (20), would enhance cytotoxicity. The data of Fig. 2B and C show that 4-HPR cytotoxicity was enhanced by the inclusion of DMS, particularly at higher 4-HPR concentrations that increased (dihydro)ceramides. In MCF-7/AdrR cells (Fig. 2B), with 3.0 μmol/L 4-HPR and 1.5 μmol/L DMS, cell killing was additive (combination index, 1.2); however, at higher concentrations (e.g., 6.0 μmol/L 4-HPR and 3.0 μmol/L DMS), cell killing was synergistic (combination index, 0.6). The addition of DMS, which was minimally cytotoxic at the concentrations tested, also enhanced the cytotoxicity of 4-HPR in HL-60 cells (Fig. 2C). For example, the addition of DMS (1.25 μmol/L) to 4-HPR (2.5 μmol/L) enhanced cell killing synergistically (combination index, 0.5). To determine what aspects of sphingolipid metabolism correlated with cell killing, we investigated pathways involved in ceramide generation and conducted detailed lipid analyses.

4-HPR has been shown to increase ceramides by the *de novo* pathway (18, 21, 30, 31). We confirmed this in MCF-7/AdrR cells by using myriocin and FB_1, inhibitors of early enzymes of sphingolipid biosynthesis, serine palmitoyltransferase and (dihydro)ceramide synthases, respectively. Either agent (FB_1, 50 μmol/L; myriocin, 0.25 μmol/L), when introduced simultaneously with 4-HPR and [^{3}H]palmitate, blocked 4-HPR–induced [^{3}H](dihydro)ceramide increase (data not shown). Next, we determined the influence of 4-HPR and DMS on sphingolipid metabolism using LC MS/MS methods for quantitative analysis. Total ceramides, without regard to molecular species, sphinganine, sphingosine, and S-1-P were measured (Table 1) after +24 and +48 hours of

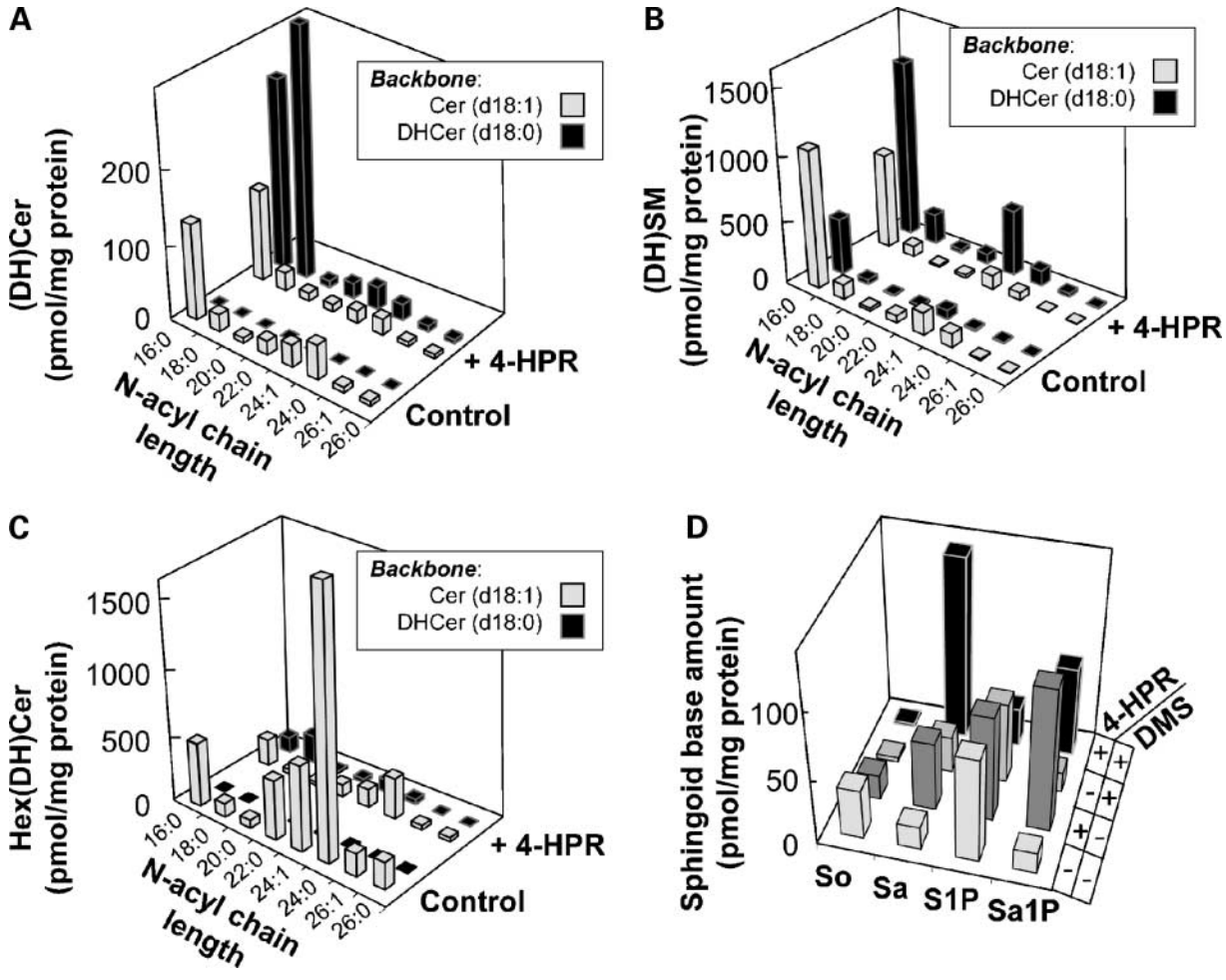

Figure 3. Sphingolipid composition of MCF-7/AdrR cells treated with vehicle, 4-HPR (5 μmol/L), or 4-HPR/DMS (5 μmol/L). After incubation for 48 h, cells were harvested and the sphingolipids analyzed by LC MS/MS with quantitation by multiple reaction monitoring for each fatty acid chain length subspecies of ceramide (*Cer*; d18:1) and dihydroceramide (*DHCer*; d18:0; **A**), and for these backbones in (dihydro)sphingomyelins [*(DH)SM*; **B**] and monohexosylceramide (**C**). The first two rows of **D** show the amounts of sphinganine (Sa), sphingosine (*So*), sphinganine 1-phosphate (Sa1-P), sphingosine 1-phosphate (S1P) in cells treated with vehicle (−) or 4-HPR (5 μmol/L; +). Also shown are the sphingoid base amounts when the cells were treated with DMS (5 μmol/L) and the combination of DMS + 4-HPR. Experimental variance was <10% for essentially all of the subspecies, but error bars have not been shown for simplicity.

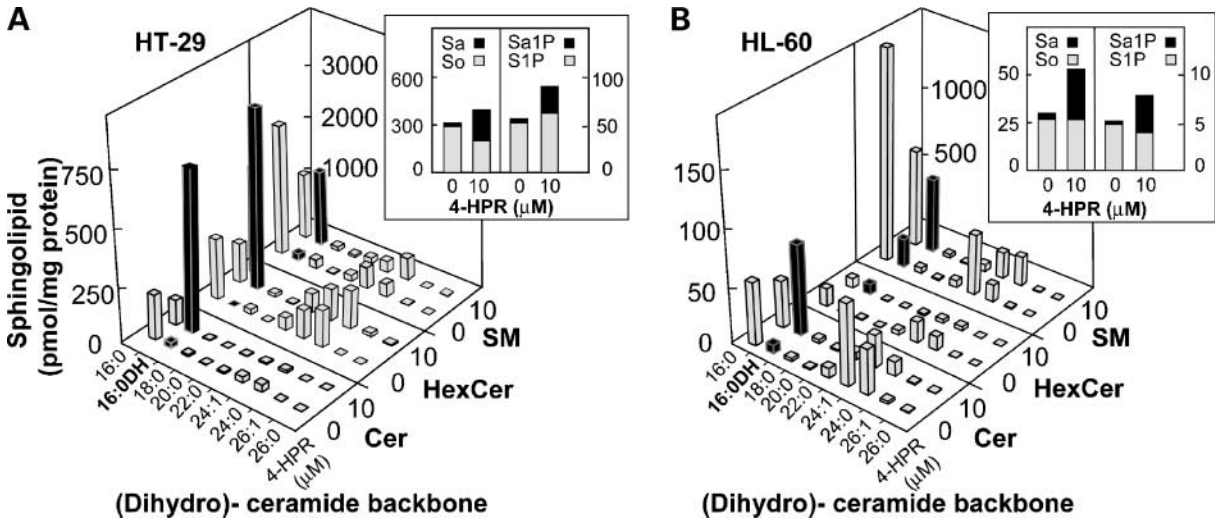

Figure 4. Sphingolipid composition of HT-29 and HL-60 cells treated with vehicle or 4-HPR. After incubation with DMSO (controls) or 4-HPR (10 μmol/L; in DMSO, 1 μL) for 24 h, the cells were harvested and analyzed by LC MS/MS. **A**, HT-29 cells. **B**, HL-60 cells. The multiple reaction monitoring protocol included one precursor/product ion pair for the major dihydroceramide (C16-DHCer), which is highlighted by labeling in black. Changes in sphingoids and sphingoid base phosphates are shown in insets. Experimental variance was < 10% for essentially all of the subspecies, but error bars have not been shown for simplicity. Cer, (dihydro)ceramides; HexCer, hexose-containing (dihydro)ceramides; SM, (dihydro)sphingomyelins. Other abbreviations as in Fig. 3.

exposures. 4-HPR alone, compared with controls, enhanced total ceramide levels dose-responsively by 2.8- and 7.7-fold at 24 and 48 hours, respectively. The 4-HPR/DMS regimen, compared with controls, elevated total cellular ceramide levels by 4.4- and 17-fold at +24 and +48 hours, respectively. Sphinganine, an early product in the *de novo* pathway, increased additively on exposure to 4-HPR, DMS, and 4-HPR/DMS. For example, at +24 hours, 4-HPR, DMS, and 4-HPR/DMS increased sphinganine levels 6-, 2.3-, and 8.7-fold, respectively, and at +48 hours, increased sphinganine levels 3.0-, 1.6-, and 8.0-fold over controls, respectively. Importantly, the 4-HPR/DMS combination promoted a more than additive increase in sphinganine at +48 hours. The levels of sphingosine were not dramatically altered by 4-HPR treatment, whereas DMS diminished sphingosine levels by 8.7-fold (11% of control) and 10.3-fold (10% of

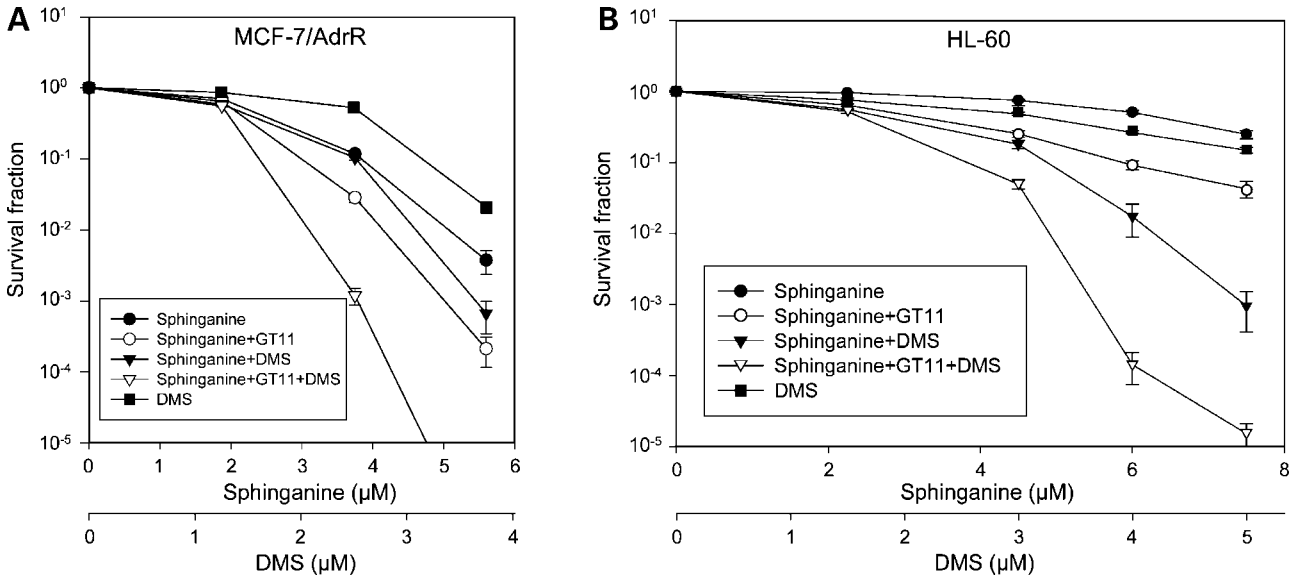

Figure 5. Dose-response of MCF-7/AdrR and HL-60 cells to sphinganine, DMS, and GT11. Cells were seeded into 96-well plates at 5,000 per well and, the following day, treated with the agents indicated. Control wells received ethanol (final concentration, 0.15%). GT11 was minimally cytotoxic at the concentration used (0.5 μmol/L). Cytotoxicity was analyzed at +72 h using DIMSCAN assay (18). **A.** MCF-7/AdrR cells. **B.** HL-60 cells: 2.25 μmol/L sphinganine + 1.5 μmol/L DMS (combination index, 1.0); 4.5 μmol/L sphinganine + 3 μmol/L DMS (combination index, 1.1); 6 μmol/L sphinganine + 4 μmol/L DMS (combination index, 0.59); 7.5 μmol/L sphinganine + 5 μmol/L DMS (combination index, 0.27).

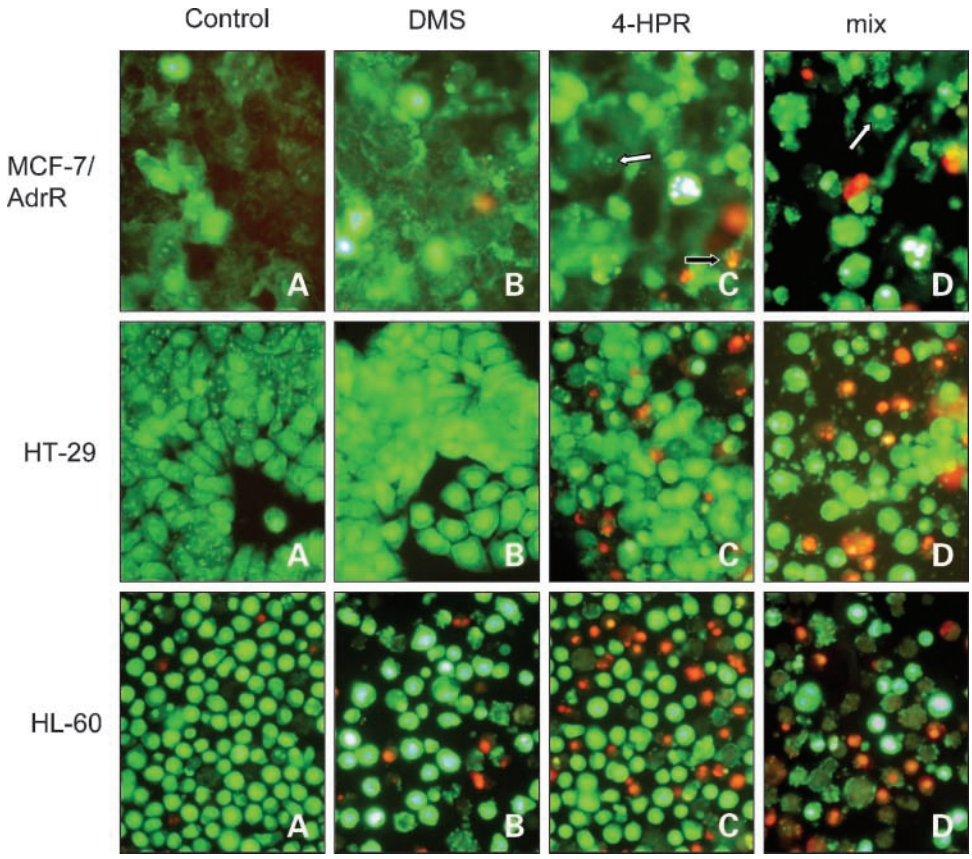

Figure 6. Effects of 4-HPR and DMS on induction of apoptosis in cancer cell lines. Apoptosis was evaluated at +48 h after treatment of MCF-7/AdrR cells (both agents at 5.0 μmol/L), HT-29 cells (DMS, 2.5 μmol/L; 4-HPR, 5.0 μmol/L), and HL-60 cells (DMS, 2.5 μmol/L; 4-HPR, 5.0 μmol/L) by fluorescent staining using SYTO-13 (0.6 μmol/L) and propidium iodide (15 μmol/L) as described in Materials and Methods. *White arrows,* apoptosis (condensed green-colored chromatin and/or fragmentation); *black arrow,* postapoptotic necrosis (orange-colored nuclear fragments.).

control) at +24 and +48 hours, respectively. At +24 hours, 4-HPR treatment diminished S1P levels by ~60%; however, by +48 hours levels were similar to controls. DMS treatment decreased relative S1P levels by ~60% at +24 hours, but S1P returned to 80% of control levels at +48 hours. The 4-HPR/DMS regimen reduced S1P levels by 68% and 63% at +24 and +48 hours, respectively, compared with control.

We next determined the molecular subspecies of sphingolipids in MCF-7/AdrR cells treated with the 4-HPR/DMS combination. After first scanning the lipid extracts to determine the species that were present, a multiple reaction monitoring protocol was used to quantify these species by comparison with internal standards (29). Desaturated ceramides were not elevated by 4-HPR. Instead, there was notable elevation in dihydroceramides, particularly the 16- and 18-carbon chain species (Fig. 3A). This was accompanied by reductions in desaturated ceramide–containing sphingomyelin (Fig. 3B) and monohexosylceramides (Fig. 3C) and elevations in the dihydroceramide backbone versions of these complex sphingolipids. It may be noteworthy that the decreases in desaturated ceramide backbone–containing sphingomyelin were more than compensated for by increases in dihydrosphingomyelin, whereas the elevation in monohexosyl-dihydroceramides did not compensate for the decreases in monohexosylceramides (compare Fig. 3B and C). Another interesting change in the MCF-7/AdrR cells treated with 4-HPR was a marked increase in sphinganine and sphinganine 1-phosphate (Sa1P), but not sphingosine or S1P (Fig. 3D, *front two rows*). These findings are intriguing because sphinganine is known to be cytotoxic (32). We speculate that Sa1P might protect from cytotoxicity when generated endogenously, although it does not seem to be protective when added exogenously although it is recognized by at least some S1P receptors (33). To explore a possible role of these sphingoid bases in the cytotoxicity of 4-HPR, we characterized the effects of DMS on S1P and Sa1P (Fig. 3D, *back two rows*). In cells treated with DMS alone, there was a small decrease in S1P that was accompanied by decrease in sphingosine; sphinganine and Sa1P were little affected by DMS. However, in the presence of DMS, 4-HPR caused a nearly 3-fold greater increase in sphinganine (for an ~9-fold increase versus the untreated control), whereas the Sa1P increase was blunted (Fig. 3D, *rows 2* and *4*). In summary, 4-HPR treatment alone caused increases in Sa1P > sphinganine and no increases in sphingosine or S1P, and in the presence of DMS, 4-HPR increased sphinganine > Sa1P and both sphingosine and S1P decreased.

The increase of cytotoxicity of the 4-HPR/DMS regimen in the multidrug resistant MCF-7/AdrR cells compared with single-agent treatment was striking (see Fig. 2B). This cytotoxicity increase seemed to correlate with sphinganine levels (Fig. 3D) but was not obviously associated

with changes in the amounts and types of more complex sphingolipids in the MCF-7/AdrR cells, as these were not found to be substantially different in cells treated with 4-HPR alone versus 4-HPR/DMS. For example, analysis of (dihydro)ceramides, (dihydro)sphingomyelin, and monohexosyl(dihydro)ceramides by LC MS/MS showed little change in the amounts of these complex lipids in cells exposed to either DMS or 4-HPR/DMS, compared with 4-HPR (data not shown; experiment conducted as described in Fig. 3D). However, a limitation of the approach used is that experiments measured steady-state sphingolipid levels at +48 hours and not the flux of total sphingolipid mass through the various pathways.

We have recently reported that 4-HPR elevates dihydroceramide in DU-145 prostate cancer cells (4) and in MOLT-4 ALL leukemia cells (19); therefore, this may be a common cancer cell response to 4-HPR. To explore this further, the effects of 4-HPR were examined using two additional human cancer cell lines, HT-29 colon cancer cells and HL-60 human promyelocytic leukemia cells. As shown in Fig. 4, for both of these cell lines, 4-HPR treatment had the same general effects on sphingolipid composition as was seen in MCF-7/AdrR cells, notably dramatic increases in dihydroceramides (shown for C16-dihydroceramide in Fig. 4A and B), as well as the presence of the dihydroceramide backbone in sphingomyelins and monohexosylglycosphingolipids. Decreases in C16-ceramides and certain other chain length ceramides and substantial increases in sphinganine and Sa1P (Fig. 4A and B, *insets*) were also determined.

Sphinganine has been reported to be cytotoxic for many transformed cells (32), but to the best of our knowledge, this has not been tested previously with multidrug-resistant cancer cells. Consistent with other types of transformed cells, sphinganine was cytotoxic in MCF-7/AdrR cells (Fig. 5A). Sphinganine is converted to dihydroceramides by dihydroceramide synthases (see Fig. 1). Interestingly, the addition of GT11, a dihydroceramide desaturase inhibitor (34), which mimicked the effect of 4-HPR on dihydroceramide desaturase, enhanced sphinganine cytotoxicity (Fig. 5A). A similar experiment conducted in HL-60 cells showed that whereas these cells were largely refractory to sphinganine, both GT11 and DMS enhanced sphinganine cytotoxicity (Fig. 5B). Sphinganine combined with DMS at 6 and 4 μmol/L, respectively, induced 98% cell kill, and the combination was synergistic (combination index, 0.6). The combination of sphinganine + GT11 + DMS showed the highest toxicity in both cell lines.

We evaluated the influence of a six-carbon cell-permeable analogue of dihydroceramide on MCF-7/AdrR cells and compared it to C6-ceramide. Cells were exposed in 96-well plates for 72 hours. Whereas C6-ceramide reduced cell viability with an EC_{50} of ~13 μmol/L, no reduction in cell viability was observed with C6-dihydroceramide at concentrations as high as 20 μmol/L (data not shown), consistent with previous reports of the minimal cytotoxicity of short-chain dihydroceramides. The specific cytotoxicity of long-chain dihydroceramides such as those increased by 4-HPR is under investigation.

Lastly, we evaluated the ability of 4-HPR and DMS to induce apoptosis in MCF-7/AdrR, HT-29, and HL-60 cells. For this, SYTO-13 and propidium iodide, two vital fluorescent dyes, were used. With these reagents, normal nuclei exhibit loose green-colored chromatin; apoptotic nuclei exhibit condensed green-colored chromatin and/or fragmentation (punctate). Postapoptotic necrosis is denoted by nuclei exhibiting the same apoptotic morphologic features, but orange colored. Apoptosis, a well-known cell death mechanism of 4-HPR, was evident in MCF-7/AdrR, HT-29, and HC-60 cells after 48-hour exposure (Fig. 6). As noted by increased nuclear fragmentation, the addition of DMS to 4-HPR greatly enhanced apoptosis in all cell lines, thus showing the potency and versatility of this binary combination. In HL-60 cells, DMS alone elicited nuclear morphology characteristic to apoptosis.

Discussion

The goal of the present study was to assess the mechanism(s) of action of 4-HPR with respect to the role of sphingolipids in the cytotoxic response using human cancer cell models. Our hope is that this information will lead to strategies to enhance the single-agent efficacy of 4-HPR and/or facilitate the design of multiagent drug combinations that contain 4-HPR as a sphingolipid species modulator. Clinical trials have shown that both acute and chronic administrations of 4-HPR to cancer patients are well tolerated (35–37). New oral and i.v. formulations of 4-HPR specifically designed to increase plasma levels and dosing intensity are currently in phase I clinical trials supported by the National Cancer Institute Rapid Access to Intervention Development program, with encouraging results.[5] In one study of clinically achievable doses in ovarian cancer patients, 4-HPR steady-state plasma levels ranged from 3.1 to 12.5 μmol/L (4-HPR capsules, 900 mg/m^2 twice daily for 7 days; ref. 38). Overall survival with plasma levels equal to 9 μmol/L was significantly higher than for those with 4-HPR levels <9 μmol/L. In a phase I study of a 4-HPR i.v. emulsion in hematologic malignancies, the emulsion showed a linear relationship of 4-HPR dose to 4-HPR plasma level obtained, with total steady-state 4-HPR plasma levels of >50 μmol/L at >905 mg/m^2/d, although free 4-HPR plasma drug levels and 4-HPR tissue levels remain to be determined (39). These studies indicate that doses evaluated *in vitro* are achievable clinically.

One mechanism whereby single agent 4-HPR has been reported to induce apoptosis and/or necrosis in cancer cells is via the increase of ceramides (21, 22, 30, 31, 40, 41). However, because many studies used less precise TLC methods that could not provide in-depth structural information, it was not known which particular

[5] B.J. Maurer, personal communication.

sphingolipid subspecies were elevated. This could be an important factor because certain chain length ceramides (i.e., C16 and C18) have been more often associated with inhibition of cell growth and induction of apoptosis (1). The specific nature of the sphingoid base backbone is also important because exogenously delivered short-chain dihydroceramides are generally held to be less bioactive than ceramides in tumor cells and in normal cells (41–43). Hence, it was of considerable surprise for us to find, using LC MS/MS to analyze the sphingolipids of MCF-7/AdrR, HL-60, and HT-29 cells, as well as DU-145 prostate and MOLT-4 ALL cancer cells, in related studies (4, 19), that 4-HPR caused large increases in dihydroceramides and more complex sphingolipids containing these saturated backbones. The elevation in dihydroceramides is likely due to stimulation of *de novo* ceramide synthesis with concurrent inhibition of dihydroceramide desaturase because studies by our lab (4) and others (44) have found that this enzymatic activity is significantly decreased by addition of 4-HPR to intact cell or *in vitro* activity assays. Therefore, because 4-HPR stimulates serine palmitoyltransferase and dihydroceramide synthase (21), inhibition of the desaturase would be predicted to cause large increases in dihydroceramides (Fig. 1).

In addition to the elevation in dihydrosphingolipids, our analyses revealed that 4-HPR also caused large increases in sphinganine and Sa1P. This is intriguing because elevation of sphinganine is known to be cytotoxic (27, 45), whereas sphingoid base 1-phosphates are mitogenic and inhibit apoptosis (20). Therefore, in addition to dihydrosphingolipids, 4-HPR increased the amount of both pro– and anti–cell death mediators. To test the hypothesis that Sa1P might interfere with the cytotoxicity of 4-HPR, DMS was used to decrease the amount of Sa1P and also decrease S1P; this resulted in additional elevation of the amount of sphinganine (Fig. 3D). The 4-HPR/DMS combination was synergistically cytotoxic in MCF-7/AdrR and HL-60 cells, and the combination elicited apoptosis in all three cell lines (Fig. 6). This suggests that sphingoid bases are among the mediators of the cellular effects of single agent 4-HPR and especially of the 4-HPR/DMS combination, particularly considering the potent cytotoxicity of exogenously added sphinganine for MCF-7/AdrR cells (Fig. 5A). Our previous studies on synergistic cytotoxicity between 4-HPR and safingol, a putative sphingosine kinase inhibitor, in solid tumor cell lines (18) support our findings in 4-HPR and DMS. Further, that HL-60 cells were largely refractory to sphinganine but vulnerable to the sphinganine/DMS combination (Fig. 5B) lends support to the antagonistic roles of sphinganine and Sa1P in the cytotoxic response to 4-HPR.

Our study, like those by other investigators using varying types of short-chain ceramide analogues, found that exogenously delivered short-chain C6-dihydroceramide was not cytotoxic. However, the biological equivalency of cell-penetrant, short-chain dihydroceramides versus native long-chain dihydroceramides is not clear. Indeed, short-chain desaturated ceramides undergo cellular uptake, hydrolysis, and reacylation to long-chain ceramides (46), and in breast cancer cell lines [^{14}C]C6-ceramide was shown to be largely converted to glucosyl[^{14}C]C6-ceramide (47). To gain insight into the cytotoxic potential of long-chain dihydroceramides, we used GT11, an inhibitor of dihydroceramide desaturase (34), in cells exposed to sphinganine, a dihydroceramide precursor (Fig. 5A and B). In both MCF-7/AdrR and HL-60 cells, the combination of sphinganine and GT11 was more cytotoxic than either agent alone. It is interesting to note that the three-drug combination of sphinganine + GT11 + DMS, which would block sphinganine phosphorylation and retard conversion of long-chain dihydroceramides to ceramides, was the most cytotoxic. These data suggest that long-chain dihydroceramides may have direct cytotoxic properties. Dihydroceramides are also known inducers of autophagy (4), a process that is both protective and lethal for cancer cells, depending on various factors (48–50). Indeed, production of S1P by sphingosine kinase is one of the factors that have been found to be important in noncytotoxic autophagy (3, 50); therefore, suppression of 4-HPR–induced Sa1P might alter the balance between ''safe'' and ''lethal'' autophagy and play a role in the synergy between 4-HPR and DMS. The advent of new formulations of fenretinide that achieve higher 4-HPR plasma levels and, presumably, increased tumor bed levels suggests that combination chemotherapies that directly manipulate sphingolipid levels to enhance cancer-cell–specific cytotoxicity may soon be clinically achievable. Further preclinical investigations of these sphingolipid pathways are, therefore, indicted.

Disclosure of Potential Conflicts of Interest

No potential conflicts of interest were disclosed.

Acknowledgments

We thank June Kawahara, Michelle Idler, Eric Morrison, Vicky Norton, Rose Ostrander, and Jessica Alvarez for compiling the typescript; and Adam Blackstone and Karen Hirsch, Ph.D., for assistance with the figures.

References

1. Ogretmen B, Hannun YA. Biologically active sphingolipids in cancer pathogenesis and treatment. Nat Rev Cancer 2004;4:604–16.

2. Fox TE, Finnegan CM, Blumenthal R, Kester M. The clinical potential of sphingolipid-based therapeutics. Cell Mol Life Sci 2006;63:1017–23.

3. Lavieu G, Scarlatti F, Sala G, et al. Regulation of autophagy by sphingosine kinase 1 and its role in cell survival during nutrient starvation. J Biol Chem 2006;281:8518–27.

4. Zheng W, Kollmeyer J, Symolon H, et al. Ceramides and other bioactive sphingolipid backbones in health and disease: lipidomic analysis, metabolism and roles in membrane structure, dynamics, signaling and autophagy. Biochim Biophys Acta 2006;1758:1864–84.

5. Senchenkov A, Litvak DA, Cabot MC. Targeting ceramide metabolism-a strategy for overcoming drug resistance. J Natl Cancer Inst 2001;93:347–57.

6. Ogretmen B, Hannun YA. Updates on functions of ceramide in chemotherapy-induced cell death and in multidrug resistance. Drug Resist Updat 2001;4:368–77.

7. Sietsma H, Veldman RJ, Kok JW. The involvement of sphingolipids in multidrug resistance. J Membr Biol 2001;181:153–62.

8. Hannun YA, Obeid LM. Mechanisms of ceramide-mediated apoptosis. Adv Exp Med Biol 1997;407:145–9.

9. Perry DK, Kolesnick RN. Ceramide and sphingosine 1-phosphate in anti-cancer therapies. Cancer Treat Res 2003;115:345 – 54.

10. Makin G, Dive C. Apoptosis and cancer chemotherapy. Trends Cell Biol 2001;11:S22 – 6.

11. Hu W, Kavanagh JJ. Anticancer therapy targeting the apoptotic pathway. Lancet Oncol 2003;4:721 – 9.

12. Scarlatti F, Bauvy C, Ventruti A, et al. Ceramide-mediated macroautophagy involves inhibition of protein kinase B and up-regulation of beclin 1. J Biol Chem 2004;279:18384 – 91.

13. Kolesnick R. The therapeutic potential of modulating the ceramide/sphingomyelin pathway. J Clin Invest 2002;110:3 – 8.

14. Liu YY, Han TY, Giuliano AE, Cabot MC. Ceramide glycosylation potentiates cellular multidrug resistance. FASEB J 2001;15:719 – 30.

15. di Bartolomeo S, Spinedi A. Differential chemosensitizing effect of two glucosylceramide synthase inhibitors in hepatoma cells. Biochem Biophys Res Commun 2001;288:269 – 74.

16. Veldman RJ, Klappe K, Hinrichs J, et al. Altered sphingolipid metabolism in multidrug-resistant ovarian cancer cells is due to uncoupling of glycolipid biosynthesis in the Golgi apparatus. FASEB J 2002;16:1111 – 3.

17. Gouaze-Andersson V, Cabot MC. Glycosphingolipids and drug resistance. Biochim Biophys Acta 2006;1758:2096 – 103.

18. Maurer BJ, Melton L, Billups C, Cabot MC, Reynolds CP. Synergistic cytotoxicity in solid tumor cell lines between *N*-(4-hydroxyphenyl)retinamide and modulators of ceramide metabolism. J Natl Cancer Inst 2000;92:1897 – 909.

19. Kong G, Wang D, Wang H, et al. Synthetic triterpenoids have cytotoxicity in pediatric acute lymphoblastic leukemia cell lines but cytotoxicity is independent of induced ceramide increase in MOLT-4 cells. Leukemia 2008;22:1258 – 62.

20. Hait NC, Oskeritzian CA, Paugh SW, Milstien S, Spiegel S. Sphingosine kinases, sphingosine 1-phosphate, apoptosis and diseases. Biochim Biophys Acta 2006;1758:2016 – 26.

21. Wang H, Maurer BJ, Reynolds CP, Cabot MC. *N*-(4-Hydroxyphenyl)-retinamide elevates ceramide in neuroblastoma cell lines by coordinate activation of serine palmitoyltransferase and ceramide synthase. Cancer Res 2001;61:5102 – 5.

22. Maurer BJ, Metelitsa LS, Seeger RC, Cabot MC, Reynolds CP. Increase of ceramide and induction of mixed apoptosis/necrosis by *N*-(4-hydroxyphenyl)-retinamide in neuroblastoma cell lines. J Natl Cancer Inst 1999;91:1138 – 46.

23. Hail N, Jr., Kim HJ, Lotan R. Mechanisms of fenretinide-induced apoptosis. Apoptosis 2006;11:1677 – 94.

24. Liscovitch M, Ravid D. A case study in misidentification of cancer cell lines: MCF-7/AdrR cells (re-designated NCI/ADR-RES) are derived from OVCAR-8 human ovarian carcinoma cells. Cancer Lett 2007;245:350 – 2.

25. Stevens VL, Owens NE, Winton EF, Kinkade JM, Jr., Merrill AH, Jr. Modulation of retinoic acid-induced differentiation of human leukemia (HL-60) cells by serum factors and sphinganine. Cancer Res 1990;50:222 – 6.

26. Lavie Y, Cao H, Bursten SL, Giuliano AE, Cabot MC. Accumulation of glucosylceramides in multidrug-resistant cancer cells. J Biol Chem 1996;271:19530 – 6.

27. Schmelz EM, Dombrink-Kurtzman MA, Roberts PC, Kozutsumi Y, Kawasaki T, Merrill AH, Jr. Induction of apoptosis by fumonisin B1 in HT29 cells is mediated by the accumulation of endogenous free sphingoid bases. Toxicol Appl Pharmacol 1998;148:252 – 60.

28. Bligh EG, Dyer WJ. A rapid method of total lipid extraction and purification. Can J Biochem Physiol 1959;37:911 – 7.

29. Merrill AH, Jr., Sullards MC, Allegood JC, Kelly S, Wang E. Sphingolipidomics: high-throughput, structure-specific, and quantitative analysis of sphingolipids by liquid chromatography tandem mass spectrometry. Methods 2005;36:207 – 24.

30. Wang H, Charles AG, Frankel AJ, Cabot MC. Increasing intracellular ceramide: an approach that enhances the cytotoxic response in prostate cancer cells. Urology 2003;61:1047 – 52.

31. Rehman F, Shanmugasundaram P, Schrey MP. Fenretinide stimulates redox-sensitive ceramide production in breast cancer cells: potential role in drug-induced cytotoxicity. Br J Cancer 2004;91:1821 – 8.

32. Stevens VL, Nimkar S, Jamison WC, Liotta DC, Merrill AH, Jr. Characteristics of the growth inhibition and cytotoxicity of long-chain (sphingoid) bases for Chinese hamster ovary cells: evidence for an involvement of protein kinase C. Biochim Biophys Acta 1990;1051:37 – 45.

33. Van Brocklyn JR, Lee MJ, Menzeleev R, et al. Dual actions of sphingosine-1-phosphate: extracellular through the Gi-coupled receptor Edg-1 and intracellular to regulate proliferation and survival. J Cell Biol 1998;142:229 – 40.

34. Triola G, Fabrias G, Dragusin M, et al. Specificity of the dihydroceramide desaturase inhibitor *N*-[(1*R*,2*S*)-2-hydroxy-1-hydroxymethyl-2-(2-tridecyl-1-cyclopropenyl)ethyl]octanamide (GT11) in primary cultured cerebellar neurons. Mol Pharmacol 2004;66:1671 – 8.

35. Rotmensz N, De Palo G, Formelli F, et al. Long-term tolerability of fenretinide (4-HPR) in breast cancer patients. Eur J Cancer 1991;27:1127 – 31.

36. Villablanca JG, Krailo MD, Ames MM, Reid JM, Reaman GH, Reynolds CP. Phase I trial of oral fenretinide in children with high-risk solid tumors: a report from the Children's Oncology Group (CCG 09709). J Clin Oncol 2006;24:3423 – 30.

37. Garaventa A, Luksch R, Lo Piccolo MS, et al. Phase I trial and pharmacokinetics of fenretinide in children with neuroblastoma. Clin Cancer Res 2003;9:2032 – 9.

38. Mohrbacher A, Gutierrez M, Murgo AJ, et al. Phase I trial of fenretinide (4-HPR) intravenous emulsion for hematologic malignancies [abstract # 2581]. American Society of Hematology Meeting; 2007.

39. Reynolds CP, Frgala T, Tsao-Wei DD, et al. High plasma levels of fenretinide (4-HPR) were associated with improved outcome in a phase II study of recurrent ovarian cancer: a study by the California Cancer Consortium. Chicago (IL): Proc ASCO; 2007. p. 287S.

40. Kalli KR, Devine KE, Cabot MC, et al. Heterogeneous role of caspase-8 in fenretinide-induced apoptosis in epithelial ovarian carcinoma cell lines. Mol Pharmacol 2003;64:1434 – 43.

41. Bielawska A, Crane HM, Liotta D, Obeid LM, Hannun YA. Selectivity of ceramide-mediated biology. Lack of activity of erythro-dihydroceramide. J Biol Chem 1993;268:26226 – 32.

42. Garcia-Ruiz C, Colell A, Mari M, Morales A, Fernandez-Checa JC. Direct effect of ceramide on the mitochondrial electron transport chain leads to generation of reactive oxygen species. Role of mitochondrial glutathione. J Biol Chem 1997;272:11369 – 77.

43. Lopez-Marure R, Gutierrez G, Mendoza C, et al. Ceramide promotes the death of human cervical tumor cells in the absence of biochemical and morphological markers of apoptosis. Biochem Biophys Res Commun 2002;293:1028 – 36.

44. Kraveka JM, Li L, Szulc ZM, et al. Involvement of dihydroceramide desaturase in cell cycle progression in human neuroblastoma cells. J Biol Chem 2007;282:16718 – 28.

45. Yu CH, Lee YM, Yun YP, Yoo HS. Differential effects of fumonisin B1 on cell death in cultured cells: the significance of the elevated sphinganine. Arch Pharm Res 2001;24:136 – 43.

46. Ogretmen BPB, Rossi M, Wood R, et al. Biochemical mechanisms of the generation of endogenous long chain ceramide in response to exogenous short chain ceramide in the A549 human lung adenocarcinoma cell line role for endogenous ceramide in mediating the action of exogenous ceramide. J Biol Chem 2002;277:12960 – 9.

47. Gouaze-Andersson V, Yu JY, Kreitenberg AJ, Bielawska A, Giuliano AE, Cabot MC. Ceramide and glucosylceramide up-regulate expression of the multidrug resistance gene MDR1 in cancer cells. Biochim Biophys Acta 2007;1771:1407 – 17.

48. Shintani T, Klionsky DJ. Autophagy in health and disease: a double-edged sword. Science 2004;306:990 – 5.

49. Kondo Y, Kanzawa T, Sawaya R, Kondo S. The role of autophagy in cancer development and response to therapy. Nat Rev Cancer 2005;5:726 – 34.

50. Lavieu G, Scarlatti F, Sala G, et al. Is autophagy the key mechanism by which the sphingolipid rheostat controls the cell fate decision? Autophagy 2007;3:45 – 7.